Optical Spectroscopic Study on Ion-Ion Recombination and Neutralization Reactions of Kr^+ with $C_6F_5Cl^-$ and Xe^+ with SF_6^-, $C_6F_6^-$, and $C_6F_5Cl^-$ in the He Flowing Afterglow

Masaharu TSUJI,[*1,2†] Hiroaki ISHIMI,[*3] Keiko UTO,[*1]
Jun-Ichiro HAYASHI[*1] and Takeshi TSUJI[*4]
[†]E-mail of corresponding author: tsuji@cm.kyushu-u.ac.jp

The positive ion-negative ion reactions of $Kr^+(^2P_{1/2,3/2})$ with $C_6F_5Cl^-$, and $Xe^+(^2P_{1/2,3/2})$ with SF_6^-, $C_6F_6^-$, and $C_6F_5Cl^-$ have been spectroscopically studied in the He flowing afterglow. KrCl* excimer and excited Kr* atoms were produced in the $Kr^+/C_6F_5Cl^-$ reaction, whereas XeF*, Xe*, and XeCl* and Xe* were formed in the Xe^+/SF_6^-, $Xe^+/C_6F_6^-$, and $Xe^+/C_6F_5Cl^-$ reactions, respectively. The branching ratios between recombination and neutralization reactions leading to RgX* (Rg = Kr, Xe, X = F, Cl) excimers and excited Rg* atoms, respectively, were found to be 0.69:0.31 for the $Kr^+/C_6F_5Cl^-$ reaction and 1.00:0.00, 0.00:1.00, and 0.89:0.11, for the Xe^+/SF_6^-, $Xe^+/C_6F_6^-$, and $Xe^+/C_6F_5Cl^-$ reactions. These results suggested that the branching ratio between recombination and neutralization reactions depends strongly on the negative ion. It was concluded that dissociation energies of target anions leading to X^- and electron affinities of target molecules play a significant role in the ion-ion recombination and neutralization reactions of Rg^+ with SF_6^-, $C_6F_6^-$, and $C_6F_5Cl^-$.
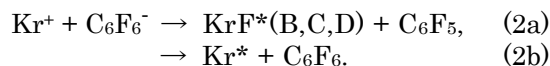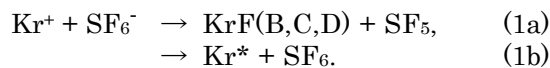
Key words: Ion-ion reaction, Flowing afterglow, Emission spectroscopy, Kr^+, Xe^+, SF_6^-, $C_6F_6^-$, $C_6F_5Cl^-$, Recombination reaction, Neutralization reaction, Branching ratio, KrCl* excimer, XeF* excimer, XeCl* excimer, Excited rare gas atoms

1. Introduction

Since reaction rate constants of ion-ion recombination reactions between positive and negative ions are extremely large due to a mutual coulombic attractive force,[1] ion-ion recombination reactions are an important loss process of ions in natural plasmas including interstellar gas clouds and in man-made plasmas such as static and flowing afterglows and laser plasmas. Although rate constants of ion-ion recombination reactions have been measured and calculated theoretically for various systems,[2-9] little work has been carried out on the measurements of product state distribution.

We have previously studied the positive ion-negative ion reactions of $Kr^+(^2P_{1/2,3/2})$ with SF_6^- and $C_6F_6^-$ in the flowing afterglow by observing product emission spectra in the vacuum ultraviolet (VUV), ultraviolet, and visible region.[10] We found that recombination reactions (1a) and (2a) leading to KrF(B,C,D) excimers and neutralization reactions (1b) and (2b) leading to excited Kr* atoms compete with each other.

$$Kr^+ + SF_6^- \rightarrow KrF(B,C,D) + SF_5, \quad (1a)$$
$$\rightarrow Kr^* + SF_6. \quad (1b)$$

$$Kr^+ + C_6F_6^- \rightarrow KrF^*(B,C,D) + C_6F_5, \quad (2a)$$
$$\rightarrow Kr^* + C_6F_6. \quad (2b)$$

The relative formation ratio of KrF*/Kr* in the $Kr^+(^2P_{1/2,3/2})/C_6F_6^-$ reaction was much smaller than that in the $Kr^+(^2P_{1/2,3/2})/SF_6^-$ reaction.

In this study, ion-ion recombination and

---

*1 Institute for Materials Chemistry and Engineering, and Research and Education Center of Green Technology
*2 Department of Molecular Science and Technology
*3 Department of Molecular Science and Technology, Graduate Student
*4 Department of Materials Science, Shimane University

neutralization reactions of $Kr^+(^2P_{1/2,3/2})$ with $C_6F_5Cl^-$ and $Xe^+(^2P_{1/2,3/2})$ with SF_6^-, $C_6F_6^-$, and $C_6F_5Cl^-$ are studied by observing RgX* and Rg* emissions (Rg = Kr, Xe and X = F, Cl) in the flowing afterglow. The branching ratios of recombination and neutralization reactions leading to RgX* excimers and excited Rg* atoms, respectively, are determined. Results obtained are compared with our previous data for the Kr^+/SF_6^- and $Kr^+/C_6F_6^-$ reactions.[10]
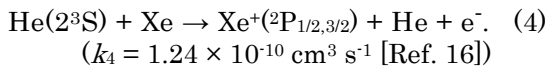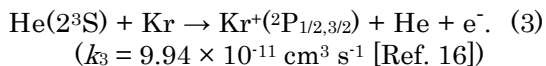
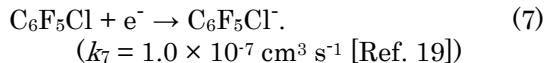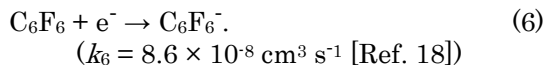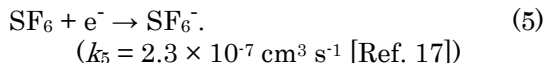## 2. Experimental

2.1 Chemicals

Gaseous and liquid samples used in this study were obtained from Japanese chemical companies: He (purity >99.9999%, Taiyo Sanso), Kr (99.995%, Nippon Sanso), Xe (99.99%, Nippon Sanso), SF_6 (99.7%, Nippon Fusso Kagaku), C_6F_6 (98%, Kishida Kagaku), and C_6F_5Cl (Kishida Kagaku, 95%). These samples were used without further purification.

2.2 Apparatus and experimental procedures

The flowing-afterglow apparatus used in this study was essentially identical with that reported previously.[10-14] We initially generated such He active species as $He(2^3S)$, He^+, and He_2^+ by a microwave discharge of high purity He gas in a He flowing afterglow at the output power of 100 W.[15] He^+ and He_2^+ ions in the discharge flow were trapped by using charged-particle collector grids placed between the discharge section and the reaction zone. Therefore, only neutral $He(2^3S)$ atoms can arrive at the reaction zone as He active species. A small amount of Kr or Xe gas was added to the He flow 10 cm downstream from the center of microwave discharge. The positive $Kr^+(^2P_{1/2,3/2})$ or $Xe^+(^2P_{1/2,3/2})$ ion was produced by the $He(2^3S)/Kr$ or $He(2^3S)/Xe$ Penning ionization.

$$He(2^3S) + Kr \rightarrow Kr^+(^2P_{1/2,3/2}) + He + e^-. \quad (3)$$
$$(k_3 = 9.94 \times 10^{-11} \text{ cm}^3 \text{ s}^{-1} \text{ [Ref. 16]})$$

$$He(2^3S) + Xe \rightarrow Xe^+(^2P_{1/2,3/2}) + He + e^-. \quad (4)$$
$$(k_4 = 1.24 \times 10^{-10} \text{ cm}^3 \text{ s}^{-1} \text{ [Ref. 16]})$$

Further 10 cm downstream from the Kr or Xe gas inlet, an electron attachment gas, SF_6, C_6F_6, or C_6F_5Cl, was added, where negative SF_6^-, $C_6F_6^-$, or $C_6F_5Cl^-$ ion was formed by a fast non-dissociative electron attachment to these three gases.

$$SF_6 + e^- \rightarrow SF_6^-. \quad (5)$$
$$(k_5 = 2.3 \times 10^{-7} \text{ cm}^3 \text{ s}^{-1} \text{ [Ref. 17]})$$

$$C_6F_6 + e^- \rightarrow C_6F_6^-. \quad (6)$$
$$(k_6 = 8.6 \times 10^{-8} \text{ cm}^3 \text{ s}^{-1} \text{ [Ref. 18]})$$

$$C_6F_5Cl + e^- \rightarrow C_6F_5Cl^-. \quad (7)$$
$$(k_7 = 1.0 \times 10^{-7} \text{ cm}^3 \text{ s}^{-1} \text{ [Ref. 19]})$$

The partial pressures in the reaction zone were 1.0 Torr (1 Torr = 133.33 Pa) for He, 5–40 mTorr for Kr or Xe, and 3–5 mTorr for SF_6, C_6F_6 and C_6F_5Cl.

The emission spectra, observed around the SF_6, C_6F_6, or C_6F_5Cl gas inlet, were dispersed in the 120–840 nm region with McPherson 218 and Spex 1250M monochromators. Photon signals from a cooled photomultiplier were analyzed with a microcomputer.

We used ionization potentials of Kr and Xe, electron affinities of SF_6, C_6F_6, and C_6F_5Cl, dissociation energies of $D(SF_5–F)$, $D(C_6F_5–F)$, and $D(C_6F_5–Cl)$, excitation energies of excimers and excited rare gas atoms reported in Refs. 20–26 for the calculations of energetics in each reaction.

3. Results and Discussion

3.1 Branching ratio of KrCl* and Kr* in the $Kr^+/C_6F_5Cl^-$ reaction

Figure 1 shows a typical emission spectrum resulting from the $Kr^+/C_6F_5Cl^-$ reaction in the 120–280 nm region. Three transitions of KrCl* excimer are identified in the 180–275 nm region. KrCl* excimer bands consists of the strong B(1/2)–X(1/2) transition in the 180–225 nm region, the weak D(1/2)–X(1/2) transition in the 180–200 nm region, and the weak broad C(3/2)–A(3/2) transition in the 225–275 nm region. Since the B, C, and D states of RgX* (Rg = rare gas atom, X = halogen atom) are strongly bound, whereas the X and A states of RgX* are repulsive,[24-26] continuous bands without vibrational structures are observed for the
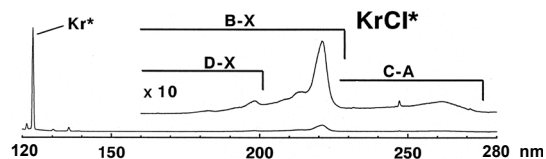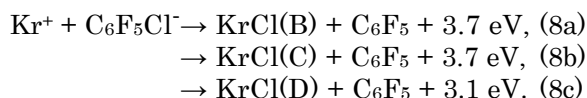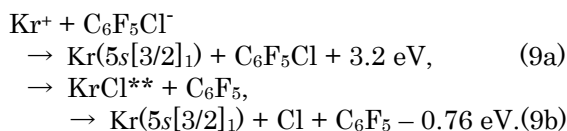

Fig. 1. Emission spectrum resulting from the $Kr^+/C_6F_5Cl^-$ reaction in the 120–280 nm region.

KrCl(B–X, D–X, C–A) bound-free transitions. The energetics for the formation of KrCl(B,C,D) from the $Kr^+/C_6F_5Cl^-$ reaction is as follows:

$$Kr^+ + C_6F_5Cl^- \rightarrow KrCl(B) + C_6F_5 + 3.7 \text{ eV}, \quad (8a)$$
$$\rightarrow KrCl(C) + C_6F_5 + 3.7 \text{ eV}, \quad (8b)$$
$$\rightarrow KrCl(D) + C_6F_5 + 3.1 \text{ eV}. \quad (8c)$$

In this study, we measured emission spectrum in the VUV region to examine whether Kr* emission resulting from neutralization reaction appears or not. A strong $Kr(5s[3/2]_1 \rightarrow 4p^6\,^1S_0)$ line is observed at 124 nm. When emission spectrum in the 300–800 nm region was observed to examine the contribution of the radiative cascade from the upper states to the $Kr(5s[3/2]_1)$ state, no Kr* lines were observed. It was therefore concluded that the $Kr(5s[3/2]_1)$ state is formed directly.
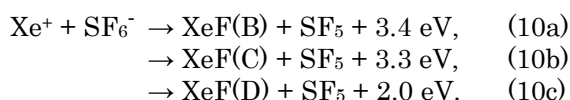
Possible mechanisms for the formation of $Kr(5s[3/2]_1)$ atoms are neutralization (9a) and predissociation of highly vibrationally excited KrCl** (9b).

$$Kr^+ + C_6F_5Cl^-$$
$$\rightarrow Kr(5s[3/2]_1) + C_6F_5Cl + 3.2 \text{ eV}, \quad (9a)$$
$$\rightarrow KrCl^{**} + C_6F_5,$$
$$\rightarrow Kr(5s[3/2]_1) + Cl + C_6F_5 - 0.76 \text{ eV}. (9b)$$

Since predissociation process (9b) is endoergic, this process is energetically excluded from possible mechanisms at thermal energy ($\approx$300 K). Based on above results, both recombination reaction leading to KrCl(B,C,D) (8a)–(8c) and neutralization process (9a) occur competitively in the $Kr^+/C_6F_5Cl^-$ reaction. The branching ratio of processes (8a)–(8c) and (9a) was determined to be 0.69:0.31 by measuring the total intensities of KrCl* and Kr* emissions.

3.2 Branching ratios of XeF* and Xe* in the reactions of Xe^+ with SF_6^-, $C_6F_6^-$, and $C_6F_5Cl^-$

When emission spectrum resulting from the Xe^+/SF_6^- reaction was measured in the 200–600 nm region, XeF(B–X,D–X,C–A) emissions were observed, as reported previously.[11]

$$Xe^+ + SF_6^- \rightarrow XeF(B) + SF_5 + 3.4 \text{ eV}, \quad (10a)$$
$$\rightarrow XeF(C) + SF_5 + 3.3 \text{ eV}, \quad (10b)$$
$$\rightarrow XeF(D) + SF_5 + 2.0 \text{ eV}. \quad (10c)$$

In this study, we measured emission spectrum in the VUV region to examine whether Xe* emission resulting from neutralization reaction appears or not.
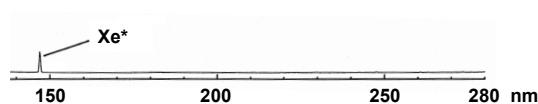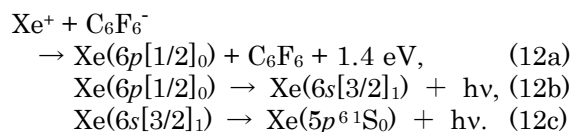

Fig. 2. Emission spectrum resulting from the $Xe^+/C_6F_6^-$ reaction in the 140–280 nm region.
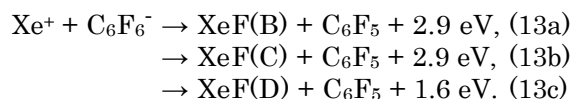
$$Xe^+ + SF_6^- \rightarrow Xe^* + SF_6. \quad (11)$$

No Xe* line arising from the Xe^+/SF_6^- reaction was observed. Thus, it was found the branching ratio of processes (10a)–(10c) and (11) is 1.00:0.00.

Figure 2 shows emission spectrum resulting from the $Xe^+/C_6F_6^-$ reaction in the 140–280 nm region, where a weak $Xe(6s[3/2]_1 \rightarrow 5p^6\,^1S_0)$ line is identified at 147 nm. When emission spectrum in the 280–830 nm was observed, a weak $Xe(6p[1/2]_0 \rightarrow 6s[3/2]_1)$ line is identified at 828 nm. It was therefore concluded that the $Xe(6s[3/2]_1)$ state is exclusively formed through radiative cascade from the upper $Xe(6p[1/2]_0)$ state.

$$Xe^+ + C_6F_6^-$$
$$\rightarrow Xe(6p[1/2]_0) + C_6F_6 + 1.4 \text{ eV}, \quad (12a)$$
$$Xe(6p[1/2]_0) \rightarrow Xe(6s[3/2]_1) + h\nu, \quad (12b)$$
$$Xe(6s[3/2]_1) \rightarrow Xe(5p^6\,^1S_0) + h\nu. \quad (12c)$$

It should be noted that no XeF(B–X,D–X,C–A) emissions were observed in the $Xe^+/C_6F_6^-$ reaction, even though they are energetically accessible.

$$Xe^+ + C_6F_6^- \rightarrow XeF(B) + C_6F_5 + 2.9 \text{ eV}, \quad (13a)$$
$$\rightarrow XeF(C) + C_6F_5 + 2.9 \text{ eV}, \quad (13b)$$
$$\rightarrow XeF(D) + C_6F_5 + 1.6 \text{ eV}. \quad (13c)$$

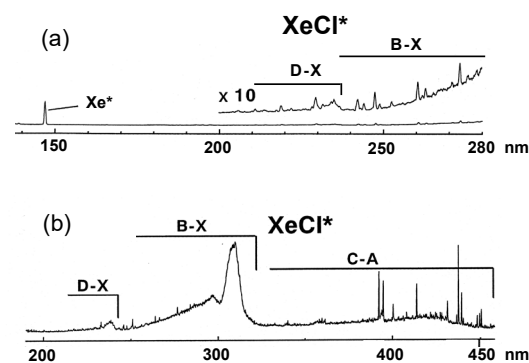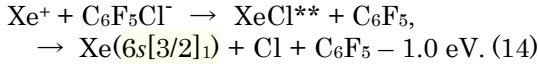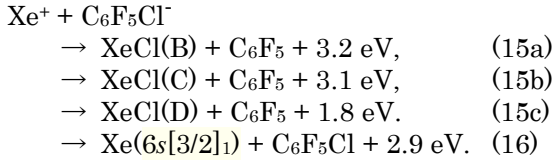Therefore, the branching ratio of processes (12a) and (13a)–(13c) is 1.00:0.00 in the

Fig. 3. Emission spectra resulting from the $Xe^+/C_6F_5Cl^-$ reaction in the (a) 140–280 nm region and (b) 200–460 nm region.

$Xe^+/C_6F_6^-$ reaction.

Figures 3a and 3b show emission spectra resulting from the $Xe^+/C_6F_5Cl^-$ reaction in the 140–280 nm region and 200–460 nm region, respectively. XeCl* excimer bands are composed of the strong B–X transition in the 240–320 nm region, the weak D–X transition in the 210–235 nm region, and the weak broad C–A transition in the 325–455 nm region. In addition, a weak $Xe(6s[3/2]_1 \rightarrow 5p^6\ {}^1S_0)$ line is observed at 147 nm. When emission spectrum in the 450–830 nm was observed, no Xe* line is observed. It was therefore concluded that the $Xe(6s[3/2]_1)$ state is produced directly in the $Xe^+/C_6F_5Cl^-$ reaction. The formation of $Xe(6s[3/2]_1)$ through predissociation of XeCl** excimer is not allowed energetically.

$$Xe^+ + C_6F_5Cl^- \rightarrow XeCl^{**} + C_6F_5,$$
$$\rightarrow Xe(6s[3/2]_1) + Cl + C_6F_5 - 1.0\ eV.\ (14)$$

Based on these facts, recombination processes (15a)–(15c) and neutralization process (16) occur competitively in the $Xe^+/C_6F_5Cl^-$ reaction.

$$Xe^+ + C_6F_5Cl^-$$
$$\rightarrow XeCl(B) + C_6F_5 + 3.2\ eV, \qquad (15a)$$
$$\rightarrow XeCl(C) + C_6F_5 + 3.1\ eV, \qquad (15b)$$
$$\rightarrow XeCl(D) + C_6F_5 + 1.8\ eV. \qquad (15c)$$
$$\rightarrow Xe(6s[3/2]_1) + C_6F_5Cl + 2.9\ eV. \quad (16)$$

The branching ratio of processes (15a)–(15c) and (16) is 0.89:0.11 in the $Xe^+/C_6F_5Cl^-$ reaction.

In Table 1 are summarized the branching ratios of RgX* excimers and Rg* atoms in the Xe^+/SF_6^-, $Xe^+/C_6F_6^-$, $Xe^+/C_6F_5Cl^-$, and $Kr^+/C_6F_5Cl^-$ reactions. For comparison,

corresponding data for the Kr^+/SF_6^- and $Kr^+/C_6F_6^-$ reactions[10] are also given. Although we reported the branching ratio of $5p[3/2]_2 + 5p[5/2]_3$: KrF(B,C,D) in the $Kr^+/C_6F_6^-$ reaction to be 0.999 : 0.001, the branching ratios of $5p[3/2]_2$ and $5p[5/2]_3$ were separately determined to be 0.454 and 0.545, respectively, in this study.

The initial formation ratios of two spin-orbit components of Kr^+ and Xe^+, $[^2P_{1/2}]/[^2P_{3/2}]$, in the Penning ionization (3) and (4) were estimated to be 0.56 for Kr^+ and 0.49 for Xe^+ from the analysis of Penning ionization electron spectra.[27] We found previously that RgF(B–X) emissions are formed highly selectively by the $Rg^+(^2P_{3/2})$ reactions, whereas RgF(D–X) emissions preferentially result from the $Rg^+(^2P_{1/2})$ reactions.[11,12] Therefore, the $[Rg^+(^2P_{1/2})]/[Rg^+(^2P_{3/2})]$ ratios can be estimated by using intensity ratios of RgX(D–X)/RgX(B–X) excimers resulting from spin-orbit state selective $Rg^+(^2P_{1/2,3/2})/C_6F_5Cl^-$ reactions. We found that the RgCl(B–X) emissions are much stronger than those of RgCl(D–X) emissions, as shown in Fig. 1 and Fig. 3(b) for the cases of $Kr^+(^2P_{1/2,3/2})/C_6F_5Cl^-$ and $Xe^+(^2P_{1/2,3/2})/C_6F_5Cl^-$ reactions. It was therefore concluded that the lower $Rg^+(^2P_{3/2})$ state is major component in the present experiments.

3.3   Reaction mechanisms for the formation of RgX* and Rg* in the reactions of Rg^+ with SF_6^-, $C_6F_6^-$, and $C_6F_5Cl^-$

The XeF* excimer formation occurs exclusively in the Xe^+/SF_6^- reaction, whereas the formation of $Xe^*(6p[1/2]_0)$ takes place selectively in the $Xe^+/C_6F_6^-$ reaction. In the

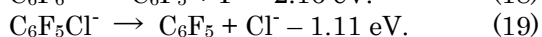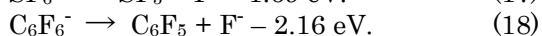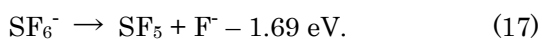**Table 1**. Branching ratios of RgX* and Rg* in the reactions of Rg^+ with SF_6^-, $C_6F_6^-$, and $C_6F_5Cl^-$.

Reaction		XeF(B,C,D)	XeCl(B,C,D)	Xe*	
				$6s[3/2]_1$	$6p[1/2]_0$
Xe^+/SF_6^-	This work	1.00		0.00	0.00
$Xe^+/C_6F_6^-$	This work	0.00		0.00	1.00
$Xe^+/C_6F_5Cl^-$	This work	0.00	0.89	0.11	0.00

Reaction		KrF(B,C,D)	KrCl(B,C,D)	Kr*		
				$5s[3/2]_1$	$5p[3/2]_2$	$5p[5/2]_3$
Kr^+/SF_6^-	Ref. 10	0.951		0.049	0.000	0.000
$Kr^+/C_6F_6^-$	Ref. 10 and This work	0.001		0.000	0.454	0.545
$Kr^+/C_6F_5Cl^-$	This work	0.00	0.69	0.31	0.000	0.000

$Xe^+/C_6F_5Cl^-$ reaction, both XeCl* excimer formation and Xe*(6s[3/2]$_1$) atom formation occur. The former XeCl* formation process is a major process, which occupies 89%. Similar tendencies are found between the branching ratios of RgX* excimer and Kr* atom in the reactions of Kr^+ with SF_6^-, $C_6F_6^-$, and $C_6F_5Cl^-$. Both KrCl* excimer and Kr*(5s[3/2]$_1$) atom are produced in the $Kr^+/C_6F_5Cl^-$ reaction. The branching ratio of KrCl* in the $Kr^+/C_6F_5Cl^-$ reaction is smaller than that of XeCl* in the $Xe^+/C_6F_5Cl^-$ reaction by 22%.

Positive ion-negative ion reactions procced through curve crossings between strongly attractive entrance ion-pair surfaces with flat exit covalent ones.[10-14] In our previous comparative study between the Kr^+/SF_6^- and $Kr^+/C_6F_6^-$ reactions,[10] we discussed a key factor which governs the branching ratio of recombination and neutralization reactions using potential-energy diagram of entrance and exit channels. We found that the magnitude of the crossing point between entrance and exit product potentials is not a significant factor in accessing the branching ratio of recombination and neutralization channels. We concluded that the dissociation energy leading to F^- anion and the electron affinity of target molecules would be more important factor in assessing the branching ratio of the two channels.

The dissociation energies of D(SF_5–F^-), D(C_6F_5–F^-), and D(C_6F_5–Cl^-) are as follows.

$$SF_6^- \rightarrow SF_5 + F^- - 1.69 \text{ eV}. \tag{17}$$
$$C_6F_6^- \rightarrow C_6F_5 + F^- - 2.16 \text{ eV}. \tag{18}$$
$$C_6F_5Cl^- \rightarrow C_6F_5 + Cl^- - 1.11 \text{ eV}. \tag{19}$$

On the other hand, electron affinities of SF_6, C_6F_6, and C_6F_5Cl provide energies required for an electron release from their anions.

$$SF_6^- \rightarrow SF_6 + e^- - 1.03 \text{ eV}. \tag{20}$$
$$C_6F_6^- \rightarrow C_6F_6 + e^- - 0.53 \text{ eV}. \tag{21}$$
$$C_6F_5Cl^- \rightarrow C_6F_5Cl + e^- - 0.75 \text{ eV}. \tag{22}$$
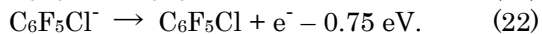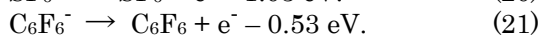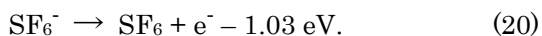
Although we used an electron affinity of 0.86 eV for C_6F_6 in our previous study,[10] more recent value of 0.53 eV[23] is employed in this study. On the basis of the above energetics for SF_6^- and $C_6F_6^-$, F^- transfer is more favorable for SF_6^-, while an electron transfer is more favorable for $C_6F_6^-$. In this study, only F^- transfer was observed in the Xe^+/SF_6^- reaction, whereas only an electron transfer was found in the $Xe^+/C_6F_6^-$ reaction, as in the cases of the Kr^+/SF_6^- and $Kr^+/C_6F_6^-$ reactions.[10] These results are consistent with the above prediction. It was thus confirmed that dissociation energies of target anions leading to F^- and electron affinities of target molecules play a significant role in the ion-ion recombination and neutralization reactions of Rg^+(Rg = Kr, Xe) with SF_6^- and $C_6F_6^-$.

The energy required for Cl^- transfer from $C_6F_5Cl^-$ is smaller than those required for F^- transfer from SF_6^- and $C_6F_6^-$. Therefore, Cl^- transfer is expected to be favorable in the $Kr^+/C_6F_5Cl^-$ and $Xe^+/C_6F_5Cl^-$ reactions. Actually, Cl^-–transfer reactions were observed as major product channels in these reactions. The electron affinity of C_6F_5Cl is just intermediate between SF_6 and C_6F_6. Therefore, electron-transfer reactions also occur as minor product channels in the $Kr^+/C_6F_5Cl^-$ and $Xe^+/C_6F_5Cl^-$ reactions.

4.　Summary and Conclusion

The $Kr^+/C_6F_5Cl^-$, Xe^+/SF_6^-, $Xe^+/C_6F_6^-$, and $Xe^+/C_6F_5Cl^-$ ion-ion mutual recombination and neutralization reactions have been spectroscopically studied in the He flowing afterglow. KrCl(B,C,D) and Kr(5s[3/2]$_1$) were produced in the $Kr^+/C_6F_5Cl^-$ reaction, whereas XeF(B,C,D), Xe(6p[1/2]$_0$), and XeCl(B,C,D) and Xe(6s[3/2]$_1$) were formed in the Xe^+/SF_6^-, $Xe^+/C_6F_6^-$, and $Xe^+/C_6F_5Cl^-$ reactions, respectively. The branching ratios of recombination and neutralization reactions were found to be 0.69:0.31 for the $Kr^+/C_6F_5Cl^-$ reaction and 1.0:0.0, 0.0:1.0, and 0.89:0.11, for the Xe^+/SF_6^-, $Xe^+/C_6F_6^-$, and $Xe^+/C_6F_5Cl^-$ reactions, respectively. These results suggested that the branching ratio between the recombination reaction leading to RgX* excimer and the neutralization reaction leading to excited Rg* atoms depends strongly on the negative ion. Results showed that F^- transfer is dominant process for SF_6^-, whereas neutralization through an electron transfer from $C_6F_6^-$ to Rg^+ is major process for $C_6F_6^-$. $C_6F_5Cl^-$ was intermediate case between SF_6^- and $C_6F_6^-$, for which both Cl^- transfer and an electron transfer occur competitively. It was concluded that dissociation energies of target anions leading to X^- and electron affinities of target molecules play a significant role in the ion-ion recombination and neutralization reactions of Rg^+(Rg = Kr, Xe) with SF_6^-, $C_6F_6^-$, and $C_6F_5Cl^-$.

References

1) D. R. Bates, *Adv. Atomic. Mol. Phys.*, 20, 1 (1985).

2) W. H. Aberth and J. R. Peterson, *Phys. Rev.*, 189, 158 (1970).

3) D. R. Bates, "*Case Studies in Atomic Physics*", Edited by E. W. McDaniel and M. R. C. McDowell, North Holland, Amsterdam, Vol. 4, p. 57 (1974).

4) D. Smith and M. J. Church, *Int. J. Mass Spectrom. Ion Phys.*, 19, 185 (1976).

5) M. J. Church and D. Smith, *J. Phys. D*, 11, 2199 (1978).

6) M. R. Flanney, *Adv. Atomic, Mol. Opt. Phys.*, 32, 117 (1994).

7) N. S. Shuman, T. M. Miller, R. Johnsen, and A. A. Viggiano, *J. Chem. Phys.*, 140, 044304 (2014).

8) J. P. Wiens, N. S. Shuman, T. M. Miller, and A. A. Viggiano, *J. Chem. Phys.*, 144, 204309 (2016).

9) M. Zauner-Wieczorek, J. Curtius, and A. Kürten, *Atmos. Chem. Phys.*, 22, 12443 (2022).

10) M. Tsuji, H. Ishimi, and Y. Nishimura, *Chem. Lett.*, 25, 515 (1996).

11) M. Tsuji, M. Furusawa, and Y. Nishimura, *Chem. Phys. Lett.*, 166, 363 (1990).

12) M. Tsuji, M. Furusawa, H. Kouno, and Y. Nishimura, *J. Chem. Phys.*, 94, 4291 (1991).

13) M. Tsuji, *Trends Phys. Chem.*, 5, 25 (1995).

14) M. Tsuji, *Houshasenkagaku*, 62, 18 (1996).

15) M. Tsuji, "*Techniques of Chemistry: Techniques for the Study of Ion Molecule Reactions; Chapter IX. Spectroscopic Probes*", Edited by J. M. Farrar and W. Saunders, Jr., John Wiley & Sons, Inc, Publishers, 489 (1988).

16) A. L. Schmeltekopf and F. C. Fehsenfeld, *J. Chem. Phys.*, 53, 2000 (1970).

17) J. C. Poutsma, N. S. Shuman, T. M. Miller, J. Troe, and A. A. Viggiano, *J. Chem. Phys.*, 152, 124302 (2020).

18) T. M. Miller, J. M. Van Doren, A. A. Viggiano, *Int. J. Mass Spectrom.*, 233, 67 (2004).

19) T. M. Miller and A. A. Viggiano, *Phys. Rev. A*, 71, 012702 (2005).

20) C. E. Moore, "*Atomic Energy Levels*," U.S. GPO, Washington D.C., *Natl. Bur. Stand.* (U.S.) Circ. 467 (1949).

21) *Atomic Spectra Database*, *NIST Standard Reference Database*, 78, Ver. 5.9. Oct. (2021).

22) Y.-R. Luo, "*Bond Dissociation Energies*", in *CRC Handbook of Chemistry and Physics*, 81th Ed., CRC Press, Boca Raton (2000).

23) *NIST Chemistry WebBook*, *NIST Standard Reference Database*, Number 69 (2022) https://doi.org/10.18434/T4D303.

24) P. J. Hay and T. H. Dunning, *J. Chem. Phys.*, 66, 1306 (1977).

25) T. H. Dunning and P. J. Hay, *J. Chem. Phys.*, 69, 134 (1978).

26) P. J. Hay and T. H. Dunning, *J. Chem. Phys.*, 69, 2209 (1978).

27) C. E. Brion, C. A. McDowell, and W. B. Stewart, *J. Electron Spectrosc.*, 1, 113 (1972/73).